Oxo Complexes of Osmium(IV) Formed via Dioxygen Activation. X-ray Structures of $[OsX(dcpe)_2]PF_6$ (X = Cl, Br), $[OsCl(\eta^2\text{-}O_2)(dcpe)_2]BPh_4$, and $[OsCl(O)(dcpe)_2]BPh_4$ (dcpe = 1,2-Bis(dicyclohexylphosphino)ethane)

Peter Barthazy, Michael Wörle,† Heinz Rüegger,‡ and Antonio Mezzetti*

Laboratory of Inorganic Chemistry, Swiss Federal Institute of Technology, ETH Zentrum, CH-8092 Zürich, Switzerland

Received March 6, 2000

Dioxygen addition to the 16-electron complexes $[OsX(P-P)_2]^+$ (**3**) gives the dioxygen adducts $[OsCl(\eta^2\text{-}O_2)(P-P)_2]^+$ (**3**), which in turn react with HCl gas to give the novel osmium(IV) oxo complexes *trans*-$[OsX(O)(P-P)_2]^+$ (**5**) (X = Cl, Br; P−P = 1,2-bis(dicyclohexylphosphino)ethane (dcpe), 1,2-bis(diethylphosphino)ethane (depe), 1,2-bis((2*R*,5*R*)-2,5-dimethylphospholano)benzene (Me-duphos)). The complexes $[OsX(dcpe)_2]^+$ (X = Cl, Br) (**3**) are studied by X-ray crystallography and are shown to have a "Y-shaped" coordination geometry in the equatorial plane. The X-ray structural analysis of $[OsCl(\eta^2\text{-}O_2)(dcpe)_2]^+$ (**4a**) reveals an exceptionally short O−O bond (1.315(5) Å). *trans*-$[OsCl(O)(dcpe)_2]^+$ (**5a**), the first oxo complex of osmium(IV) investigated crystallographically, exhibits a long Os−O distance of 1.834(3) Å. The reactivity of **4** and **5** as oxidants is described. The dioxygen complex **4a** transfers one oxygen atom to PPh_3 (to give Ph_3PO) or oxidizes iodide ions to triiodide ions in the presence of anhydrous HCl. In both reactions, the corresponding oxo species **5a** is quantitatively formed as the only metal-containing product. Oxo complexes **5** are surprisingly stable and unreactive toward standard reducing agents such as phosphines.

Introduction

Despite its enormous potential, the use of molecular oxygen in transition-metal-catalyzed oxidation reactions is relatively rare.[1] Rather than dioxygen, most industrial processes exploit partially reduced forms of this molecule, e.g., peroxides, as well as catalysts based on metal centers in high oxidation states, often with d^0 or d^2 configurations, which easily form oxo complexes.[2] Nature instead uses processes where the metal centers are in low oxidation states, typically with d^6 configurations, and operates with the most readily available oxidant, i.e., dioxygen.[3] As several natural systems are based on the heme ferryl moiety, much effort has been directed toward developing biomimetic catalytic systems based on iron porphyrin complexes.[4] Replacement of the central atom with other members of the iron triad along with retention of the d^6 electronic configuration of the central atom offers an opportunity to vary the catalytic species. This approach was developed by Groves in his pioneering work on dioxygen activation by ruthenium porphyrin complexes[5] and has found applications in catalytic oxidation reactions.[6] However, because of the intrinsic difficulties associated with dioxygen activation,[1] advancements in this area have been much slower than those for alternative methods utilizing single-oxygen donors as oxidants in "shunt" pathways, such as those in Mn−salen catalytic systems.[7,8]

Despite the large variety of transition metals and ligands employed, all catalytic processes cited above have a number of features in common. The active species is often a five-coordinate complex $[MXL_4]$ containing four ligands L (often incorporated in chelating ligands favoring a planar geometry). The ligand X trans to the active site fine-tunes the reactivity of the system. The catalytic cycle is generally thought to involve an oxo species of the type $[MX(O)L_4]^+$. However, although the involvement of oxo complexes[2] in olefin epoxidation[9] and alkane hydroxylation[10] reactions is an established fact, well-documented examples of the formation of oxo complexes from molecular

* Corresponding author. E-mail: mezzetti@inorg.chem.ethz.ch.

† X-ray structures.

‡ 2D NMR studies.

(1) (a) Ebner, J.; Riley, D. In *Active Oxygen in Chemistry*; Foote, C. S., Valentine, J. S., Greenberg, A., Liebman, J. F., Eds.; Blackie Academic and Professional Publishers: London, 1995; Chapter 6. (b) See also refs 1a−f in ref 16 below.

(2) (a) Nugent, W. A.; Mayer, J. M. *Metal-Ligand Multiple Bonds*; Wiley: New York, 1988. (b) See also refs 3b−f in ref 16 below.

(3) (a) Ho, R. Y. N.; Liebman, J. F.; Valentine, J. S. In *Active Oxygen in Biochemistry*; Valentine, J. S., Foote, C. S., Greenberg, A., Liebman, J. F., Eds.; Blackie Academic and Professional Publishers: London, 1995. (b) See also refs 2b−f in ref 16 below.

(4) (a) Sheldon, R. A., Ed. *Metalloporphyrins in Catalytic Oxidations*; Dekker: New York, 1994. (b) Montanari, F., Casella, L., Eds. *Metalloporphyrins Catalyzed Oxidations*; Kluwer: Dordrecht, The Netherlands, 1994. For seminal papers, see: (c) Balch, A. L.; Chan, Y. W.; Cheng, R. S.; LaMar, G. N.; Latos, B.; Grazinsky, L.; Denner, M. W. *J. Am. Chem. Soc.* **1984**, *106*, 7779 and references therein.

(5) (a) Groves, J. T.; Quinn, R *J. Am. Chem. Soc.* **1985**, *107*, 5790. (b) Groves, J. T.; Quinn, R. *Inorg. Chem.* **1984**, *23*, 3844. (c) Groves, J. T.; Ahn, K. H. *Inorg. Chem.* **1987**, *26*, 3831.

(6) Selected papers: (a) Bailey, C. L.; Drago, R. S. *J. Chem. Soc., Chem. Commun.* **1987**, 179. (b) Lai, T. S.; Zhang, R.; Cheung, K. K.; Kwong, H. L.; Che, C. M. *Chem. Commun.* **1998**, 1583. (c) Neumann, R.; Dahan, M. *Nature* **1997**, *388*, 353. (d) Neumann. R.; Dahan, M. *J. Am. Chem. Soc.* **1998**, *120*, 11969.

(7) Jacobsen, E. N. In *Catalytic Asymmetric Synthesis*; Ojima, I., Ed.; VCH Publishers: New York, 1993; Chapter 4.2.

(8) Ito, Y. N.; Katsuki, T. *Bull. Chem. Soc. Jpn.* **1999**, *72*, 603.

(9) Representative papers: (a) Dobson, J. C.; Seok, W. K.; Meyer, T. J. *Inorg. Chem.* **1986**, *25*, 1513. (b) Che, C. M.; Li, C. K.; Tang, W. T.; Yu, W. Y. *J. Chem. Soc., Dalton Trans.* **1992**, 3153. (c) Goldstein, A. S.; Beer, R. H.; Drago, R. S. *J. Am. Chem. Soc.* **1994**, *116*, 2424. (d) Stultz, L. K.; Binstead, R. A.; Reynolds, M. S.; Meyer, T. J. *J. Am. Chem. Soc.* **1995**, *117*, 2520 and ref 1 therein. (e) Lai, T. S.; Kwong, H. L.; Zhang, R.; Che, C. M. *J. Chem. Soc., Dalton Trans.* **1998**, 3559.

10.1021/ic0002420 CCC: $19.00
Published on Web 09/28/2000

Scheme 1

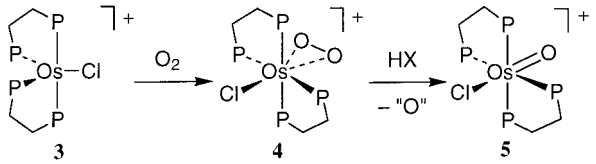

Chart 1

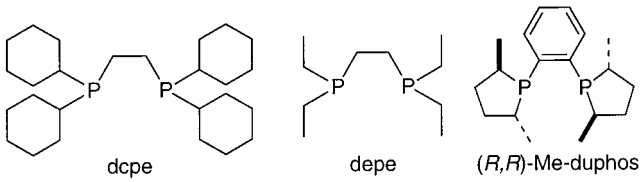

oxygen are rare in nonbiomimetic systems of the iron triad.[5,11] Indeed, most oxo complexes of ruthenium and osmium are formed by oxidation of coordinated water[12] or oxene transfer from a terminal oxidant.[4,13]

We recently found that the five-coordinate, 16-electron complexes $[OsX(dcpe)_2]^+$, **3** (X = H, Cl; dcpe = 1,2-bis(dicyclohexylphosphino)ethane),[14] activate molecular oxygen,[15] and that the resulting complex *trans*-$[OsCl(\eta^2\text{-}O_2)(dcpe)_2]^+$ (**4a**) forms the oxo species *trans*-$[OsCl(O)(dcpe)_2]^+$ (**5a**) (Scheme 1).[16] Complexes **3**−**5** belong to the series $[OsXO_nP_4]^+$, which features a variable number of oxygen atoms *n* (*n* = 0, 1, 2) with the same ligand set. These species share all the commonalities mentioned above, as they are five-coordinate complexes of the iron triad, contain an ancillary ligand X that tunes their electronic properties, and include an oxo species formed from molecular oxygen. We show herein that this chemistry can be generalized to other five-coordinate complexes $[OsX(P{-}P)_2]^+$ (**2**) (X = Cl, Br; P−P = diphosphine; Chart 1) and report their reactions with O_2 to give *trans*-$[OsX(\eta^2\text{-}O_2)(P{-}P)_2]^+$ (**4**) and, eventually, the oxo complexes *trans*-$[OsX(O)(P{-}P)_2]^+$ (**5**).

Scheme 2

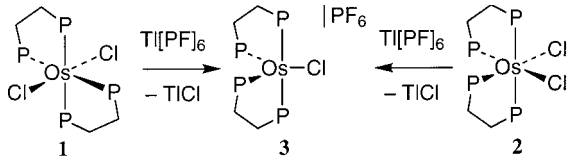

Results and Discussion

The Six-Coordinate Complexes $[OsX_2(P{-}P)_2]$. The six-coordinate complexes *trans*-$[OsX_2(P{-}P)_2]$ (**1**) and *cis*-$[OsX_2(P{-}P)_2]$ (**2**) are the precursors for the five-coordinate, 16-electron species $[OsX(P{-}P)_2]^+$ (**3**). By a variation of the published procedures, the dcpe[14] and depe (depe = 1,2-bis(diethylphosphino)ethane)[17] derivatives *trans*-$[OsX_2(P{-}P)_2]$ (P−P = dcpe, X = Cl (**1a**), Br (**1b**); P−P = depe, X = Cl (**1c**)) were prepared by ligand metathesis from $[OsX_2(PPh_3)_3]$[18] and the appropriate diphosphine ligand (2 equiv) in refluxing toluene. However, this synthetic method failed with Me-duphos (Me-duphos = (−)-1,2-bis((2*R*,5*R*)-2,5-dimethylphospholano)benzene),[19] giving a monosubstituted binuclear species, most likely $[(Me\text{-}duphos)(PPh_3)Os(\mu\text{-}Cl)_3Os(PPh_3)(Me\text{-}duphos)]Cl$, instead of the disubstituted mononuclear complex. Therefore, *cis*-$[OsCl_2(depe)_2]$ (**2c**) and *cis*-$[OsCl_2(Me\text{-}duphos)_2]$ (**2d**) were prepared by heating $[(PEt_2Ph)_3Os(\mu\text{-}Cl)_3Os(PEt_2Ph)_3]Cl$ with the neat diphosphine ligand.[17] In this series, the Me-duphos derivative **2d** is new. It shows two pseudotriplets (AA′XX′ spin system) in the ^{31}P NMR spectrum, indicating that a single diastereomer (either Δ or Λ) is formed.

The Five-Coordinate Complexes $[OsX(P{-}P)_2]PF_6$. The five-coordinate dcpe derivatives are easily prepared by reacting *trans*-$[OsX_2(dcpe)_2]$ (X = Cl (**1a**), Br (**1b**)) with a strong halide scavenger (Scheme 2). Thus, **1a,b** smoothly form $[OsCl(dcpe)_2]PF_6$ ([**3a**]PF_6) and $[OsBr(dcpe)_2]PF_6$ ([**3b**]PF_6) upon addition of $TlPF_6$. When dry, the five-coordinate species [**3a,b**]PF_6 are air-stable in the solid state for months.

In the case of the least bulky diphosphine, depe, dissociation of chloride from *trans*-$[OsCl_2(depe)_2]$ (**1c**) does not occur under the above conditions, whereas the more labile *cis*-$[OsCl_2(depe)_2]$ (**2c**) reacts with $TlPF_6$ in CH_2Cl_2 or $CHCl_3$. However, instead of the 16-electron species $[OsCl(depe)_2]^+$ (**3c**), the dioxygen complex $[OsCl(\eta^2\text{-}O_2)(depe)_2]^+$ (**4c**) is isolated when standard Schlenk techniques are employed under argon. The putative intermediate $[OsCl(depe)_2]^+$ is so reactive toward traces of O_2 that we were not able to observe it by monitoring the reaction between *cis*-$[OsCl_2(depe)_2]$ and $TlPF_6$ with ^{31}P NMR spectroscopy in CD_2Cl_2 solutions under argon. Thus, in view of the extreme reactivity of **3c** and its structural analogy to **3a,b,d**, its isolation was not further pursued.

In the case of Me-duphos, *cis*-$[OsCl_2(Me\text{-}duphos)_2]$ (**2d**) smoothly reacts with $TlPF_6$, giving $[OsCl(Me\text{-}duphos)_2]PF_6$ ([**3d**]PF_6). The new compound was characterized by ^{31}P and ^1H NMR spectroscopy and elemental analysis. The ^{31}P room-temperature NMR spectrum, consisting of two sharp triplets at δ 76.1 and 42.6 (J = 5.5 Hz), suggests that the complex has a stereochemically rigid TBP structure and is present as a single diastereomer (either Δ or Λ) under these conditions.

In general, halide dissociation is apparently favored in the sterically crowded dcpe complexes **1a,b**. In the other cases, the

(10) Representative papers: (a) Groves, J. T.; Nemo, T. E. *J. Am. Chem. Soc.* **1983**, *105*, 6243. (b) Goldstein, A. S.; Drago, R. S. *J. Chem. Soc., Chem. Commun.* **1991**, 21. (c) Bailey, A. J.; Griffith, W. P.; Savage, P. D. *J. Chem. Soc., Dalton Trans.* **1995**, 3537.
(11) (a) Bourgault, M.; Castillo, A.; Esteruelas, M. A.; Oñate, E.; Ruiz, N. *Organometallics* **1997**, *16*, 636. (b) Molina-Svendsen, H.; Bojesen, G.; McKenzie, C. J. *Inorg. Chem.* **1998**, *37*, 1981. (c) Camenzind, M. J.; James, B. R.; Dolphin, D. *J. Chem. Soc., Chem. Commun.* **1986**, 1137. (d) Hay-Motherwell, R. S.; Wilkinson, G.; Hussain-Bates, B.; Hursthouse, M. B. *Polyhedron* **1993**, *12*, 2009.
(12) See, for instance: (a) Takeuchi, K. J.; Thompson, M. S.; Pipes, D. W.; Meyer, T. J. *Inorg. Chem.* **1986**, *25*, 1845. (b) Dobson, J. C.; Takeuchi, K. J.; Popes, D. W.; Geselowitz, D. A.; Meyer, T. J. *Inorg. Chem.* **1986**, *25*, 2357. (c) Pipes, D. W.; Meyer, T. J. *Inorg. Chem.* **1986**, *25*, 4042. (d) Che, C. M.; Lai, T. F.; Wong, K. Y. *Inorg. Chem.* **1987**, *26*, 2289. (e) Marmion, M. E.; Takeuchi, K. J. *J. Am. Chem. Soc.* **1988**, *110*, 1472. (f) Che, C. M.; Cheng, W. K.; Yam, V. W. W. *J. Chem. Soc., Dalton Trans.* **1990**, 3095. (g) Cheng, C. C.; Goll, J. G.; Neyhart, G. A.; Welch, T. W.; Singh, P.; Thorp, H. H. *J. Am. Chem. Soc.* **1995**, *117*, 2970. (h) Cheng, W. C.; Yu, W. Y.; Zhu, J.; Cheung, K. K.; Peng, S. M.; Poon, C. K.; Che, C. M. *Inorg. Chim. Acta* **1996**, *242*, 105. (i) Catalano, V. J.; Heck, R. A.; Immoos, C. E.; Öhman, A.; Hill, M. G. *Inorg. Chem.* **1998**, *37*, 2150.
(13) See, for instance: (a) Leung, T.; James, B. R.; Dolphin, D. *Inorg. Chim. Acta* **1983**, *79*, 180. (b) Aoyagi, K.; Yukawa, Y.; Shimizu, K.; Mukaida, M.; Takeuchi, T.; Kakihana, H. *Bull. Chem. Soc. Jpn.* **1986**, *59*, 1493. (c) Leung, W. H.; Che, C. M. *J. Am. Chem. Soc.* **1989**, *111*, 8812.
(14) Mezzetti, A.; Del Zotto, A.; Rigo, P. *J. Chem. Soc., Dalton Trans.* **1990**, 2515.
(15) Mezzetti, A.; Zangrando, E.; Del Zotto, A.; Rigo, P. *J. Chem. Soc., Chem. Commun.* **1994**, 1597.
(16) Barthazy, P.; Wörle, M.; Mezzetti, A. *J. Am. Chem. Soc.* **1999**, *121*, 480.
(17) Chatt, J.; Hayter, R. G. *J. Chem. Soc.* **1961**, 896.
(18) Hoffman, P. R.; Caulton, K. G. *J. Am. Chem. Soc.* **1975**, *97*, 4221.
(19) For synthesis and application of Me-duphos, see, for instance: Burk, M. J.; Gross, M. F.; Harper, T. G.; Kalberg, C. S.; Lee, J. R.; Martinez, J. P. *Pure Appl. Chem.* **1996**, *68*, 37.

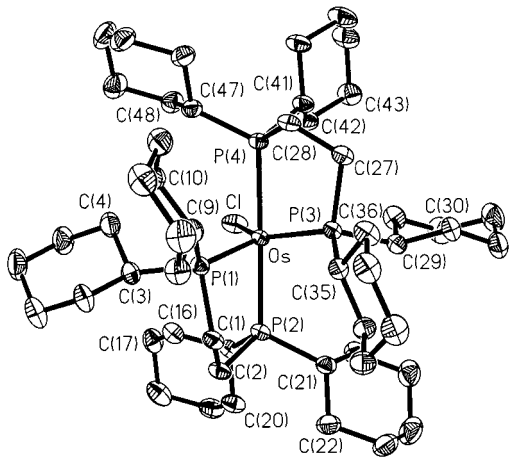

Figure 1. ORTEP view of $[OsCl(dcpe)_2]^+$ (**3a**) (30% probability ellipsoids). Selected bond distances (Å) and angles (deg): Os−Cl, 2.371(1); Os−P(1), 2.282(1); Os−P(3), 2.321(1); Os−P(2), 2.422(1); Os−P(4), 2.417(1); Cl−Os−P(1), 122.38(4); P(1)−Os−P(3), 92.58(4); Cl−Os−P(2), 88.05(4); P(1)−Os−P(4), 102.06(4); Cl−Os−P(3), 144.86(4); P(2)−Os−P(3), 101.50(4); Cl−Os−P(4), 85.78(4); P(2)−Os−P(4), 173.75(4); P(1)−Os−P(2), 82.08(4); P(3)−Os−P(4), 83.10(4).

more labile cis isomer **2** has to be used, exploiting the stronger trans effect of P as compared to Cl. The reactivity trend also suggests that the increasing basicity of the P−P ligand labilizes the halide, as observed for *trans*-$[OsCl_2(dcpe)_2]$ as compared to *trans*-$[OsCl_2(dppe)_2]$ (dppe = 1,2-bis(diphenylphosphino)-ethane). The latter species, which contains a less basic and less bulky diphosphine, does not react with $TlPF_6$, and the corresponding five-coordinate complex has been prepared from *cis*-$[OsCl_2(dppe)_2]$.[20] Steric and electronic effects apparently cooperate in stabilizing the Lewis-acidic 16-electron complexes containing the more basic and more bulky phosphines.

X-ray Structures of $[OsX(dcpe)_2]PF_6$ (X = Cl, Br). The five-coordinate nature of **3a** and **3b** was confirmed by X-ray analysis (Figure 1 and Figure S1 (Supporting Information)). Selected interatomic distances and angles of **3a** and **3b** are given in the caption to Figure 1 and in Table S2 (Supporting Information), respectively. The five-coordinate cations $[OsX(dcpe)_2]^+$ (X = Cl (**3a**), Br (**3b**)) have a Y-shaped, distorted trigonal bipyramidal structure, similar to that found in $[OsCl(dppe)_2]^+$,[21] as well as in the ruthenium analogues with dcpe[22] and other diphosphines.[23,24] This is as expected for π-stabilized 16-electron complexes.[25] The "Y-plane" is further distorted, with two largely different P−Os−X angles, as already observed in the ruthenium analogues.[22−24] Support for the role played by the π-donation from the chloride ligand comes from the Os−Cl distance of 2.371(1) Å, which is ca. 0.06 Å shorter than those in *trans*-$[OsCl_2(dppe)_2]$ (2.434(1) Å).[26,27] Similarly, the Os−Br distance in the bromo derivative **3b** is 2.481(2) Å, shorter than the 2.5738(6) Å distances in the reference compound *trans*-$[OsBr_2(dppe)_2]$.[28] Taking into account the unsaturated nature of these complexes, the axial Os−P distances in both **3a** and **3b** appear exceptionally long with respect to literature values.[21,26,29] An interesting feature in both **3a** and **3b** is the envelope conformation of the chelate rings with the flap on a C atom.

Reaction of $[OsX(P-P)_2]PF_6$ with O_2. The 16-electron species **3a,b** reacted quantitatively with O_2 in CH_2Cl_2, forming the dioxygen complexes $[OsX(\eta^2\text{-}O_2)(dcpe)_2]^+$ (X = Cl (**4a**), Br (**4b**)) within hours. The depe derivative $[OsCl(\eta^2\text{-}O_2)(depe)_2]^+$ (**4c**) was prepared directly from six-coordinate **2c** by reaction with $TlPF_6$ and O_2 in CH_3OH. The light green complexes **4a**−**c** were characterized by ^{31}P and ^1H NMR spectroscopy, mass spectrometry (FAB^+), and elemental analysis. Although the ν(O−O) stretching band was unassignable owing to the crowding of the 800−900 cm^{-1} IR spectral region, the X-ray structure of **4a** reported below gives definitive evidence of the η^2-O_2 linkage. The ^{31}P NMR spectra of **4a**−**c** consist of one sharp singlet in the range δ +10 to −10, consistent with rapid internal reorientation rendering all P atoms equivalent. In contrast, the ^{31}P NMR spectra of the related complexes $[MH(\eta^2\text{-}O_2)(P-P)_2]$ (M = Ru, Os) show broad signals at room temperature, possibly due to the hindered propeller-like rotation of the η^2-O_2 ligand.[15,30,31]

The dioxygen complex $[OsCl(\eta^2\text{-}O_2)(depe)]^+$ (**4c**) is probably the cationic species observed by Chatt and Hayter upon dissolution of *cis*-$[OsCl_2(depe)_2]$ in water.[17] In the series, the Me-duphos derivative $[OsCl(Me\text{-}duphos)_2]^+$ (**3d**) is the least reactive toward O_2. Upon exposure to air of a $CDCl_3$ solution, the five-coordinate complex **3d** remains unchanged to a great extent and no diamagnetic η^2-O_2 complex is formed, as indicated by the ^{31}P NMR spectrum. The ^1H NMR spectrum of the solution indicates that traces (~1%) of a paramagnetic complex are formed, which we tentatively formulate as the corresponding oxo complex by analogy with the other $[OsX(O)(P-P)_2]^+$ species (see below). The latter probably derives from an undetected dioxygen adduct present at low concentration in equilibrium with **3d**. Finally, for the dppe complex, no reaction with O_2 was observed.[20]

X-ray Structure of $[OsCl(\eta^2\text{-}O_2)(dcpe)_2]BPh_4$ ([4a]BPh_4). X-ray-quality crystals of [**4a**]BPh_4 were grown from CH_2Cl_2/Pr^iOH. The complexes $[OsBr(\eta^2\text{-}O_2)(dcpe)_2]^+$ (**4b**) and $[OsCl(\eta^2\text{-}O_2)(depe)_2]^+$ (**4c**) decomposed to the oxo complexes during the crystallization process. This prevented growing crystals of their salts with $[PF_6]^-$, $[BPh_4]^-$, or $[BAr_4]^-$ (BArF, Ar = 3,5-bis(trifluoromethyl)phenyl).

The formally seven-coordinate cation $[OsCl(\eta^2\text{-}O_2)(dcpe)_2]^+$ can be described as a distorted pentagonal bipyramid, with two P atoms, the Cl atom, and the two O atoms approximately in the equatorial plane and with two mutually trans axial P atoms (Figure 2, Table S3 (Supporting Information)).[32] The Os−Cl

(20) Maltby, P. A.; Schlaf, M.; Steinbeck, M.; Lough, A.; Morris, R. H.; Klooster, W. T.; Koetzle, T. F.; Srivastava, R. C. *J. Am. Chem. Soc.* **1996**, *118*, 5396.
(21) Lough, A. J.; Morris, R. H.; Schlaf, M. *Acta Crystallogr., Sect. C* **1996**, *52*, 2193.
(22) Mezzetti, A.; Del Zotto, A.; Rigo, P.; Bresciani Pahor, N. *J. Chem. Soc., Dalton Trans.* **1989**, 1045.
(23) Chin, B.; Lough, A. J.; Morris, R. H.; Schweitzer, C. T.; D'Agostino, C. *Inorg. Chem.* **1994**, *33*, 6278.
(24) Batista, A. A.; Centeno Cordeiro, L. A.; Oliva, G. *Inorg. Chim. Acta* **1993**, *203*, 185.
(25) (a) Caulton, K. G. *New J. Chem.* **1994**, *18*, 25. (b) Riehl, J. F.; Jean, Y.; Eisenstein, O.; Pélissier, M. *Organometallics* **1992**, *11*, 729. (c) Johnson, T. J.; Folting, K.; Streib, W. E.; Martin, J. D.; Huffman, J. C.; Jackson, S. A.; Eisenstein, O.; Caulton, K. G. *Inorg. Chem.* **1995**, *34*, 488 and references therein.
(26) Levason, W.; Champness, N. R.; Webster, M. *Acta Crystallogr., Sect. C* **1993**, *49*, 1884.
(27) A mean value of 2.435(9) Å is found for five complexes of the type *trans*-$[OsCl_2(PPhR_2)_4]$, as retrieved in the Cambridge Structural Database.
(28) Lough, A. J.; Morris, R. H.; Schlaf, M. *Z. Kristallogr.* **1995**, *210*, 973.
(29) Orpen, A. G.; Brammer, L.; Allen, F. H.; Kennard, O.; Watson, D. G.; Taylor, R. *J. Chem. Soc., Dalton Trans.* **1989**, S1.
(30) Jiménez-Tenorio, M.; Puerta, M. C.; Valerga, P. *Inorg. Chem.* **1994**, *33*, 3515.
(31) Martelletti, A.; Gramlich, V.; Zürcher, F.; Mezzetti, A. *New J. Chem.* **1999**, 199.

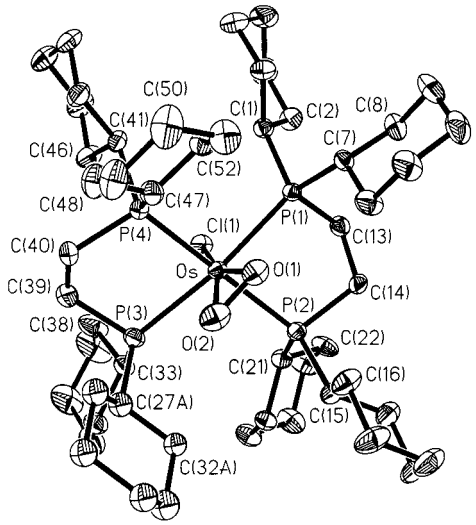

Figure 2. ORTEP view of *trans*-[OsCl(η^2-O_2)(dcpe)$_2$]$^+$ (**4a**) (30% probability ellipsoids).

Table 1. O−O and Os−O Bond Distances (Å) in [OsX(η^2-O_2)(P−P)$_2$]PF_6

	O−O	Os−O	ref
[OsCl(η^2-O_2)(dcpe)$_2$]PF_6	1.315(5)	2.006(3), 2.041(4)	this work
[OsH(η^2-O_2)(dcpe)$_2$]PF_6	1.45(1)	2.045(8), 2.037(8)	15
[OsH(η^2-O_2)(dppe)$_2$]PF_6	1.430(5)	2.061(4), 2.064(3)	33a

distance in the (formally seven-coordinate) **4a** (2.380(1) Å) is similar to that in five-coordinate **3a** (2.371(1) Å), whereas the Os−P distances are even longer than those in **3a,b**. The Os−P_4 arrangement shows a tetrahedral distortion, with the P(1) and P(3) atoms bent away from the coplanar dioxygen ligand (P(1)−Os−P(3) = 162.46(4)°). The axial P atoms are only slightly bent toward the dioxygen (P(2)−Os−P(4) = 175.91(4)°). Both chelate rings show an envelope conformation with the flap on a C atom.

Despite structural analogies, **4a** displays a much shorter O−O distance (1.315(5) Å) than [OsH(η^2-O_2)(P−P)$_2$]$^+$ (dcpe,[15] 1.45(1) Å; dppe,[33a] 1.430(5) Å; Table 1) and among the shortest ever found for a dioxygen complex.[29,34] Unfortunately, the Os−O distances are not a reliable probe of the Os−O bond strengths in **4a**, as the η^2-coordination mode of the dioxygen ligand is slightly distorted. Thus, the Os−O(2) distance is longer by 0.035(4) Å than Os−O(1) and the O(2)−O(1)−Os angle (72.5(2)°) is larger than O(1)−O(2)−Os (69.6(2)°). Comparison with [OsH(η^2-O_2)(P−P)$_2$]$^+$ (Table 1) shows an enhanced interaction between Os and one of the O atoms of η^2-O_2. Although these features invite speculation about distortion of the η^2-coordination toward η^1, their magnitudes are so small that they could be the effect of crystal packing as well.

Bonding in [MX(η^2-O_2)(P−P)$_2$]$^+$. Examples of dioxygen adducts of d^6 complexes of Ru(II)[30,31,35] and Os(II)[33,36] have been increasing in number, in particular since the recent discovery of [RuH(η^2-O_2)(P−P)$_2$]$^+$.[30] Most of these new η^2-O_2 derivatives are complexes of the type [MH(η^2-O_2)(P−P)$_2$]$^+$ (M = Ru, Os)[30−33] or [Ru(η^2-O_2)(Cp*)(P−P)]$^+$ (Cp* = C_5Me_5).[35] The present investigation contributes to the assessment of the electronic requirements for dioxygen activation by relatively electron-rich but coordinatively unsaturated Ru(II) and Os(II) complexes of the [MX(P−P)$_2$]$^+$ series. In this class of compounds, the osmium derivatives show a higher tendency to bind O_2 than the ruthenium analogues. As the five-coordinate complexes [MX(P−P)$_2$]$^+$ generally react rapidly with both neutral and anionic donors, such as halide, CO, H_2, and nitriles,[14,22,37] this is probably a thermodynamic effect, as supported by the following considerations.

Dioxygen adducts of ruthenium are formed only when several strong σ-donors (the hydride and basic P−P ligands) enhance the electron density at the metal. Thus, the five-coordinate [RuH(P−P)$_2$]$^+$ complexes form [RuH(η^2-O_2)(P−P)$_2$]$^+$ (P−P = dcpe[31] or 1,2-bis(diisopropylphosphino)ethane[30] (dippe)), whereas the chloro analogue [RuCl(dcpe)$_2$]$^+$ is stable in solutions exposed to air for short periods of time and does not form a (detectable) dioxygen adduct.[22] In the case of [OsX(dcpe)$_2$]$^+$, O_2 activation occurs also when less basic X and P−P ligands are combined, as in [OsH(dppe)$_2$]$^+$ [33a] and [OsCl(dcpe)$_2$]$^+$.[15] Indeed, the higher energy of the d orbitals of Os as compared to Ru favors the shift of electron density from the metal to the dioxygen ligand that stabilizes the M(η^2-O_2) linkage. The effect of the donor properties of the anionic ligand X is clearly visible in the series [OsX(η^2-O_2)(P−P)$_2$]$^+$, where the O−O distance increases on going from chloride (a weak donor) to hydride (a strong donor) (Table 1). In this class of compounds, the chloro derivatives [OsCl(η^2-O_2)(P−P)$_2$]$^+$ (**4a**−**c**) reported herein are the dioxygen complexes that are stabilized by the least basic ligands. However, some stable dioxygen adducts of osmium are formed even in the presence of a π-acid ligand, as in [OsHCl(η^2-O_2)(CO)(PR_3)$_2$] (R = c-C_6H_{11}, Pr^i).[36b]

Besides the nature of the metal M (M = Ru or Os) and the donor properties of the ligand X (X = halide or H), the electronic and steric properties of the diphosphine fine-tune the reactivity of [MX(P−P)$_2$]$^+$ toward O_2. As described above, the reactivity of the five-coordinate species [OsCl(P−P)$_2$]$^+$ toward dioxygen increases with increasing basicity and decreasing steric bulk of the P−P ligand along the series dppe < Me-duphos ≪ dcpe < depe.

The structural data available for [MX(η^2-O_2)(P−P)$_2$]$^+$ (M = Ru, Os; X = Cl, H) in the solid state and in solution provide further insight into the bonding in **4a**−**c**, taking into account that the η^2-O_2 ligand is a π-acceptor and the chloride a weak π-donor. The P_{eq}−Os−P_{eq} angle is much larger in **4a** (162.46(4)°) than in the hydride analogue [OsH(η^2-O_2)(dcpe)$_2$]$^+$ (136.3(1)°). As the steric crowding in chloro derivatives **4** is higher than that in the hydride analogues, this effect is more likely electronic than steric. For the related [MH(η^2-H_2)(P−P)$_2$]$^+$

(32) This is largely formal and implies that **4b** could be described as a peroxo complex of Os(IV). However, the alternative description as a six-coordinate dioxygen complex of Os(II) (featuring a distorted octahedral coordination) seems more appropriate in view of the short O−O distance and is normally used throughout this paper.

(33) (a) Bartucz, T. Y.; Golombek, A.; Lough, A. J.; Maltby, P. A.; Morris, R. H.; Ramachandran, R.; Schlaf, M. *Inorg. Chem.* **1998**, *37*, 1555. (b) Tenorio, M. J.; Puerta, M. C.; Salcedo, I.; Valerga, P. *J. Organomet. Chem.* **1998**, *564*, 21.

(34) Hill, H. A.; Tew, D. G. In *Comprehensive Coordination Chemistry*; Wilkinson, G., McCleverty, J. A., Eds.; Pergamon: Oxford, U.K., 1987; Vol. 2, p 318.

(35) Other η^2-O_2 complexes of Ru(II): (a) Kirchner, K.; Mauthner, K.; Mereiter, K.; Schmid, R. *J. Chem. Soc., Chem. Commun.* **1993**, 892. (b) De los rios, I.; Tenorio, M. J.; Padilla, J.; Puerta, M. C.; Valerga, P. *J. Chem. Soc., Dalton Trans.* **1996**, 377. (c) Sato, M.; Asai, M. *J. Organomet. Chem.* **1996**, *508*, 121. (d) Takahashi, Y.; Hikichi, S.; Akita, M.; Moro-oka, Y. *Chem. Commun.* **1999**, 1491. (e) Jia, G. C.; Ng, W. S.; Chu, H. S.; Wong, W. T.; Yu, N. T.; Williams, I. D. *Organometallics* **1999**, *18*, 3597.

(36) (a) Moers, F. G.; ten Hoedt, R. W. M.; Langhout, J. P. *J. Inorg, Nucl. Chem.* **1974**, *36*, 2279. (b) Esteruelas, M. A.; Sola, E.; Oro, L. A.; Meyer, U.; Werner, H. *Angew. Chem., Int. Ed. Engl.* **1988**, *27*, 1563. (c) For related species, see: Maddock, S. M.; Rickard, C. E. F.; Roper, W. R.; Wright, L. J. *J. Organomet. Chem.* **1996**, *510*, 267.

(37) Mezzetti, A.; Del Zotto, A.; Rigo, P.; Farnetti, E. *J. Chem. Soc., Dalton Trans.* **1991**, 1525.

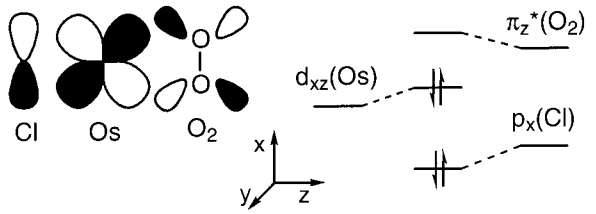

Figure 3. Partial (π-bonding) correlation diagram of the Cl−Os−η^2-O_2 fragment. Only the d_{xz} orbital has the correct symmetry for interacting with $\pi^*(O_2)$.

complex, it has been shown that the bending of two trans P atoms away from the dihydrogen ligand enhances the d_π-(M)→$\sigma^*(\eta^2\text{-}H_2)$ back-bonding.[38] This is because closing the equatorial P−Ru−P angle rehybridizes the d_{xz} orbital and raises its energy. Such a distortion is necessary in $[OsH(\eta^2\text{-}O_2)(dcpe)_2]^+$, where it improves the overlap with the π^* orbitals of O_2. In $[OsCl(\eta^2\text{-}O_2)(P{-}P)_2]$, closing one P−Ru−P angle is both unfavorable (because Cl is larger than H) and unnecessary, as the d_{xz} orbital is destabilized by the p_π orbital of the chloro ligand (Figure 3).[25] This is consistent with a weaker $d_\pi(Os)\rightarrow\pi^*$-$(\eta^2\text{-}O_2)$ binding component in **4a** than in $[OsH(\eta^2\text{-}O_2)(dcpe)_2]^+$ due to Cl being an overall weaker donor than hydride, as discussed above for the O−O and Os−O bond distances.

Variable-temperature NMR spectroscopy data support the above interpretation. Thus, the hydride analogues $[MH(\eta^2\text{-}O_2)(P{-}P)_2]^+$ (M = Ru, Os) show fluxional behavior in solution that is possibly due to the hindered propeller-like rotation of the η^2-O_2 ligand.[15,30,31] Their room-temperature ^{31}P NMR spectra show two broad humps that resolve into two pseudotriplets at low temperature. In contrast, the ^{31}P NMR spectra of the halo derivatives **4a**−**c** consist of one sharp singlet, indicating rapid rotation of η^2-O_2 on the NMR time scale due to lower energy barriers. This is contrary to expectation based on steric arguments and consistent with a larger $d_\pi(Os)\rightarrow\pi^*(\eta^2\text{-}O_2)$ binding component in chloro derivative **4a** than in $[OsH(\eta^2\text{-}O_2)(dcpe)_2]^+$.

The overall bonding pattern in the Cl−Os−$(\eta^2\text{-}O_2)$ moiety features a three-orbital, four-electron push−pull interaction between the chloro ligand and the dioxygen ligand analogous to the case of the Cl−M−CO moiety (Figure 3).[25] Accordingly, the Os−Cl distance in the formally seven-coordinate **4a** (2.380-(1) Å) is similar to that in the five-coordinate **3a** (2.371(1) Å). This is again contrary to the expectation based on steric effects and suggests that π-donation plays similar roles in both complexes.

In conclusion, the stronger Os−O bonds (and weaker O−O bond) in $[OsH(\eta^2\text{-}O_2)(P{-}P)_2]^+$ than in **4a** are due to hydride being a much stronger donor than Cl. As the Os→$(\eta^2\text{-}O_2)$ electron transfer is mediated by a π-effect, the $d_\pi(Os){-}\pi^*(O_2)$ overlap is maximized by the distortion of the equatorial P−M−P angle in the hydride complexes and by the $d_\pi(Os){-}p_\pi(Cl)$ four-electron destabilization in the case of **4**. The weaker Os−$(\eta^2\text{-}O_2)$ bonding and smaller $d_\pi{-}\pi^*$ overlap in **4** are possibly reflected in the distortion of the η^2-coordination toward η^1. This could explain the unusual reactivity of **4** as compared to the hydride analogues.

Reactivity of $[OsX(\eta^2\text{-}O_2)(P{-}P)_2]^+$. We investigated the reversibility of dioxygen addition to five-coordinate **3a**. Photolysis of **4a** (Xe lamp) in CH_2Cl_2 solution gives small amounts of five-coordinate **3a** (20%) together with other (uncharacterized) products. Heating under vacuum mainly produces dcpe dioxide. A similar behavior has been observed for $[OsH(\eta^2\text{-}O_2)(dcpe)_2]^+$.[15] Complex **4a** reacts slowly with carbon monoxide in CH_2Cl_2 solution, but ^{31}P NMR spectroscopy and stripping of the effluent gases in aqueous $Ba(OH)_2$ indicated that neither the carbonyl complex $[OsCl(CO)(dcpe)_2]^+$ nor CO_2 was formed.

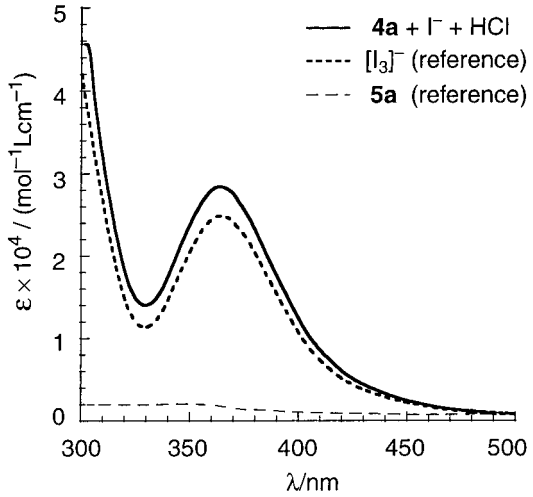

Figure 4. UV−visible monitoring of the reaction of **4a** with I^- in the presence of anhydrous HCl.

All of the dioxygen complexes **4a**−**c** are stable in the solid state, but decomposition to the oxo species *trans*-$[OsX(O)(P{-}P)_2]^+$ slowly occurs in CH_2Cl_2 solution. Simple storing of **4a**−**c** in CH_2Cl_2 solution yields the corresponding oxo complexes within 3 d. As independent experiments show that traces of acids greatly accelerate this reaction, we conclude that the reaction is triggered by traces of HCl formed by the decomposition of the chlorinated solvent over time (Scheme 1) or, alternatively, by traces of water incorporated during the preparation of **4**. Accordingly, as the $[PF_6]^-$ anion is always associated with small amounts of acids (or water), changing the anion Y^- in $[OsCl(P{-}P)_2]Y$ to $[BPh_4]^-$ or $[BAr_4]^-$ substantially increases the stability of the dioxygen complex. In contrast, $[OsH(\eta^2\text{-}O_2)(dcpe)_2]^+$ is stable in solution for longer periods of time.[15]

Neither the fate of the "lost" oxygen atom nor the mechanism of this reaction could be assessed. However, we rule out that the above reaction occurs by dissociation of O_2 from $[OsCl(\eta^2\text{-}O_2)(dcpe)_2]^+$ (**4a**) followed by formation of a peroxo-bridged intermediate,[3,6c,d] as O_2 coordination in **4a** is essentially irreversible, as discussed above, and five-coordinate **3a** does not react with the dioxygen complex **4a**.[16]

Oxidation Reactions with $[OsX(\eta^2\text{-}O_2)(P{-}P)_2]^+$ (4). The oxygen-transfer reactivity of **4a** with a number of substrates was studied. The test reactions were generally performed with $[OsCl(\eta^2\text{-}O_2)(dcpe)_2]^+$ (**4a**), but **4b** and **4c** showed similar reactivity when used in selected instances. [**4a**]BPh_4 oxidizes I^- (as $[NBu_4]I$) to triiodide, forming *trans*-$[OsCl(O)(dcpe)_2]^+$ (**5a**) in the presence of anhydrous HCl in CH_2Cl_2 according to eq 1. Monitoring of the reaction by UV−visible spectroscopy

$$[OsCl(\eta^2\text{-}O_2)(dcpe)_2]^+ + 3I^- + 2H^+ \rightarrow \textit{trans}\text{-}[OsCl(O)(dcpe)_2]^+ + I_3^- + H_2O \quad (1)$$

at 365 nm shows quantitative formation of $[I_3]^-$ and **5a** based on the absorbance trace of the reaction after correction for the absorbance of the oxo complex (Figure 4). The ^{31}P NMR spectrum of the reaction solution indicates quantitative disappearance of **4a**, whereas only the typical signals of **5a** are visible

(38) (a) Van Der Sluys, L. S.; Eckert, J.; Eisenstein, O.; Hall, J. H.; Huffman, J. C.; Jackson, S. A.; Koetzle, T. F.; Kubas, G. J.; Vergamini, P. J.; Caulton, K. G. *J. Am. Chem. Soc.* **1990**, *112*, 4831. (b) Maseras, F.; Koga, N.; Morokuma, K. *Organometallics* **1994**, *13*, 4008.

in the ^{1}H NMR spectrum. No reaction occurs without acid. Complex **4a** also oxidizes triphenylphosphine in the presence of HCl under argon (eq 2). The stoichiometry of reaction 2 is

$$[OsCl(\eta^2\text{-}O_2)(dcpe)_2]^+ + [Ph_3PH]Cl \rightarrow \textit{trans}\text{-}[OsCl(O)(dcpe)_2]^+ + Ph_3PO + HCl \quad (2)$$

well-defined, as $[Ph_3PH]Cl$ is added to **4a** (1:1 mole ratio) to give **5a** and Ph_3PO in almost quantitative yields, as measured by ^{31}P NMR spectroscopy. The reaction is complete within 10 min, and the coordinated diphosphines are not oxidized.[39]

Acid-promoted oxygen transfer has been proposed for other peroxo complexes.[1,40] In contrast to what is observed for M(η^2-O_2) complexes (M = Pt, Rh),[41] it seems unlikely that reaction 1 involves acid hydrolysis of **4a**, since the use of aqueous HCl gives yet unidentified products instead of **5a** and extraction of freshly prepared CH_2Cl_2 solutions of **5a** with aqueous titanyl sulfate does not reveal the presence of H_2O_2. Finally, **5a** does not re-form **4a** upon treatment with H_2O_2.

The oxidation of a number of organic substrates has been attempted. Complex **4a** does not epoxidize olefins (styrene) or quinone-like substrates (menadione), oxidize aldehydes (benzaldehyde) or alcohols (Pr^{i}OH, *tert*-butyl alcohol, CH_3OH), or hydroxylate alkanes (adamantane). In contrast, the dioxygen ligand of the ruthenium analogue [RuH(η^2-O_2)(dcpe)$_2$] displays moderate nucleophilic behavior and oxidizes aldehydes to the corresponding carboxylic acids.[31] With TCNE an immediate reaction occurs, but the TCNE radical anion is formed instead of the epoxide. We also tested whether **5a** shows haloperoxidase reactivity in the presence of bromide ions.[42] However, the acidic hydrolysis of the dioxygen complex **4a** in the presence of [NBu$_4$]-Br and 1,3,5-trimethoxybenzene or 2,3-dimethoxytoluene does not give the corresponding brominated derivatives (not even traces). This also disfavors the possibility that HOCl is formed in the reaction of **4a** with HCl (Scheme 1).

***trans*-[OsX(O)(P−P)$_2$]BPh$_4$.** The osmium(IV) complexes $[OsX(O)(P{-}P)_2]^+$ (X = Cl, P−P = dcpe, **5a**; X = Br, P−P = dcpe, **5b**; X = Cl, P−P = depe, **5c**) were prepared from the corresponding dioxygen complexes **4a**−**c** and fully characterized. As mentioned above, the d^4 oxo complexes **5a**−**c** are formed by oxygen transfer from the dioxygen adducts **4a**−**c** (Scheme 1) and the reaction is accelerated by gaseous HCl. The light green or brownish complexes **5a**−**c** are stable in the solid state and in solution. The Me-duphos analogue [OsCl(O)(Me-duphos)$_2$]$^+$ is formed only in traces, as discussed above. We have previously reported that **5a** is paramagnetic with an effective magnetic moment μ_{eff} of 3.05 μ_B at 300 K,[16] a value near the spin-only value for two unpaired electrons. This is explained by the molecular orbital ordering of octahedral oxo complexes with a d^4 configuration based on C_{4v} symmetry as discussed by Mayer (Figure 5).[43] In the case of the d^4 complexes $[OsX(O)(P{-}P)_2]^+$, two d electrons fill the d_{xy} orbital, and the remaining two occupy the two degenerate d_{xz} and d_{yz} orbitals with parallel spins.

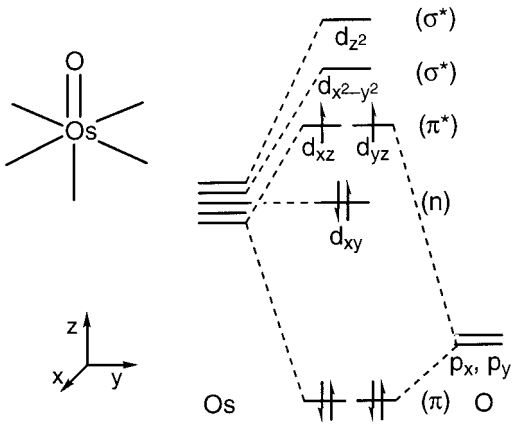

Figure 5. Partial correlation diagram of a d^4 [Os(O)L$_5$] complex.

Table 2. ^{1}H and ^{13}C NMR Data (Obtained in $CDCl_3$) for trans-[OsCl(O)(depe)$_2$]BPh$_4$ ([**5c**])BPh$_4$)

assignt[a]	δ(^{1}H)	R_2(^{1}H),[b] s^{-1}	δ(^{13}C)
CH_3(Cl)	1.5	45	−26.6
CH_3(O)	29.0	240	+34.2
CH_2(Cl)	6.9, −4.1	195, 350	−122.2
CH_2(O)	34.0, 12.3	320, 635	+173.8
CH_2(BB)	15.1, 8.1	155, 205	−85.4

[a] (Cl) and (O) denote the chloride and oxo hemispheres, respectively; (BB) denotes the diphosphine backbone. [b] Transverse relaxation rates R_2 estimated from line widths.

NMR Spectroscopy. Although no ^{31}P NMR signals can be observed (at least at room temperature), the ^{1}H and ^{13}C NMR spectra are sufficiently resolved in the diamagnetic areas and feature well-defined paramagnetic regions with relatively small isotropic shifts. Most of the signals could be assigned by a combination of one- and two-dimensional NMR techniques (Table 2). In the depe derivative *trans*-[OsCl(O)(depe)$_2$]$^+$ (**5c**), there are two inequivalent methyl groups belonging to the two hemispheres in which the oxo and the chloro substituents reside, respectively. On the basis of the assumptions (i) that most of the unpaired spin density is located either on the oxo ligand or between it and the metal and (ii) that the dipolar term dominates the relaxation behavior of the adjacent protons, we assign the slowly relaxing methyl protons resonating in the diamagnetic region of the spectrum at δ 1.5 to the group in the Cl hemisphere.

Despite the considerable transverse relaxation rates R_2 (Table 2) of the diastereotopic protons in the ethyl CH_2 groups, it proved possible to relate these to their respective CH_3's by means of a 2D TOCSY experiment. The backbone CH_2 protons are consequently assigned to the remaining two signals. All ^{13}C resonances were assigned on this basis by means of ^{1}H−^{13}C 2D-heteronuclear multiple-quantum coherence spectroscopy. It is interesting to note that the chemical shifts of the carbons residing in the oxo hemisphere are isotropically shifted toward higher frequency, whereas those of the carbons belonging to the chloride hemisphere and the chelate backbone are below the TMS frequency.

The dcpe derivatives **5a** and **5b** are completely analogous in structure and spectroscopic properties to **5c**. However, the interpretation process is more demanding in view of 12 and 22 inequivalent C and H atoms to be assigned, requiring the use of 2D methods. A contour plot of a section of the ^{1}H−^{13}C heteronuclear multiple-quantum coherence spectrum for *trans*-[OsBr(O)(dcpe)$_2$]BPh$_4$ ([**5b**]BPh$_4$) (Figure 6) in $CDCl_3$ at room temperature shows the wide spread of shifts in the carbon dimension. Indeed, with the exception of that of one α-carbon,

(39) Although [OsCl(Me-duphos)$_2$]$^+$ (**3d**) probably forms a very labile dioxygen adduct, PPh_3 is not oxidized in the presence of **3d** (1 equiv) under O_2 in $CDCl_3$.

(40) (a) van Asselt, A.; Trimmer, M. S.; Henling, M. S.; Bercaw, J. E. *J. Am. Chem. Soc.* **1988**, *110*, 8254 and ref 12 therein. (b) Conte, V.; Di Furia, F.; Moro, S. *J. Mol. Catal. A: Chem.* **1997**, *120*, 93.

(41) Selected papers: (a) Sen, A.; Halpern, J. *J. Am. Chem. Soc.* **1977**, *99*, 8337. (b) Bhaduri, S.; Casella, L.; Ugo, R.; Raithby, P. R.; Zuccaro, C.; Hursthouse, M. B. *J. Chem. Soc., Dalton Trans.* **1979**, 1624.

(42) Butler, A. *Coord. Chem. Rev.* **1999**, *187*, 17.

(43) Mayer, J. M.; Thorn, D. L.; Tulip, T. H. *J. Am. Chem. Soc.* **1985**, *107*, 7454.

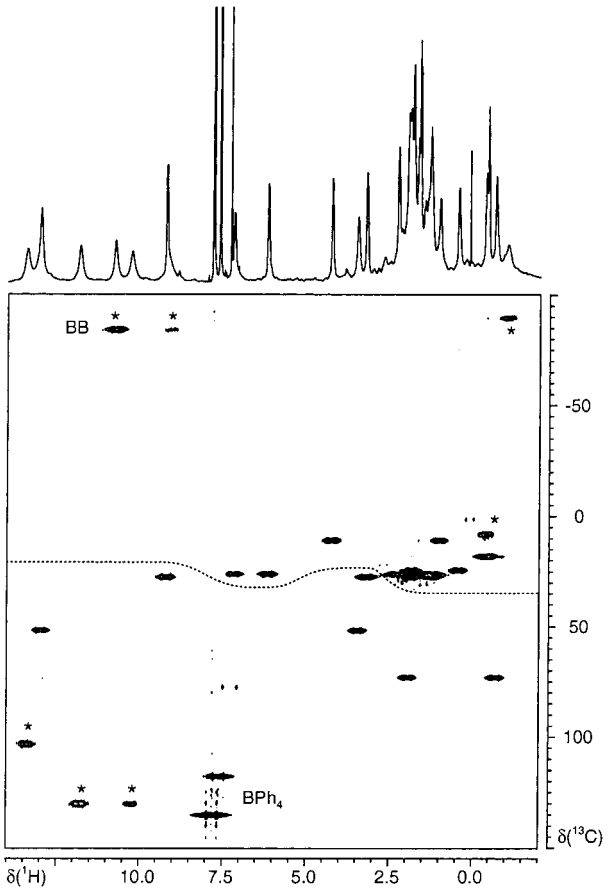

Figure 6. $^{1}H-^{13}C$ heteronuclear multiple-quantum coherence spectrum of [**5b**]BPh_4. Cross-peaks labeled with an asterisk are vertically expanded by a factor of 8; BB denotes the chelate backbone resonances. The dashed wavy line separates signals assigned to ^{1}H and ^{13}C nuclei in the two hemispheres (see text).

all resonances can be unambiguously assigned. It is again to be noted that the signals belonging to carbons in the two different hemispheres of the complex are in well-separated shift regions, whereas no such distinction can be made for the respective hydrogens. This allows structural assignments, as the ^{13}C chemical shifts of both (equivalent) C atoms of the chelate backbone are in the negative range as are those of the α-carbons of the cyclohexyl groups in the chloride hemisphere ($^{\alpha}CH(Cl)$, Table S4 (Supporting Information)). Indeed, the chelate ring present in the solid phase for **5a** exhibits an envelope conformation with a tip into this part of the molecule (see below).

X-ray Structure of [5a]BPh_4. Crystals of *trans*-[OsCl(O)(dcpe)$_2$]BPh_4 ([**5a**]BPh_4) were grown from CH_2Cl_2/Pr^{i}OH. An ORTEP view of **5a** is shown in Figure 7, and structural data are provided in Table S5 (Supporting Information). The complex cation features a slightly distorted octahedral geometry with an O(1)−Os−Cl angle of 175.1(1)°. The OsP_4 arrangement shows a tetrahedral distortion with P(1) and P(3) below the mean plane (both by −0.12 Å) and P(2) and P(4) above it (both by 0.09 Å). In agreement with the higher oxidation state of **5a**, the Os−P distances are significantly shorter than those in **4a**. The bite angles of about 82° are normal for dcpe. As already observed for **3a,b** and **4a**, the chelate rings have an envelope conformation. The Os, P(1), P(2), and C(14) atoms are nearly coplanar (±0.04 Å), and C(13) is displaced 0.71 Å from their mean plane toward Cl. In the second chelate ring, Os, P(3), P(4), and C(39) are coplanar within ±0.1 Å and C(40) is displaced 0.44 Å from their mean plane in the Cl hemisphere.

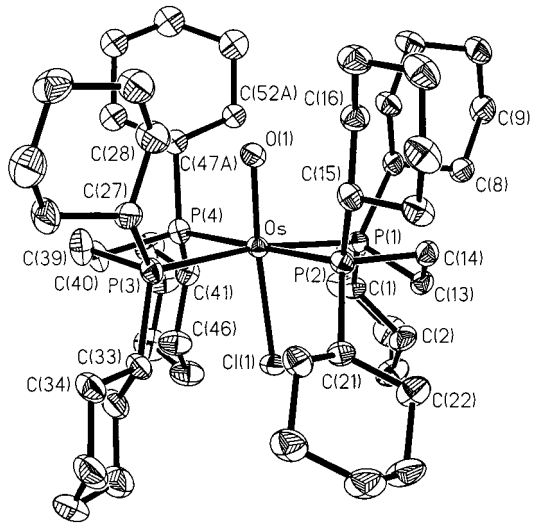

Figure 7. ORTEP view of *trans*-[OsCl(O)(dcpe)$_2$]$^+$ (**5a**) (30% probability ellipsoids).

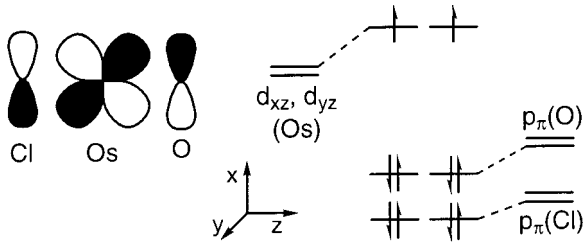

Figure 8. Correlation diagram of the Cl−Os=O fragment.

The Os−oxo linkage deserves discussion. The Os−O(1) distance in **5a** (1.834(3) Å) is much longer than those in osmium(VI) oxo complexes (ca. 1.72 Å),[2,29,44] e.g., in the (*E*)-styryl complex [OsCl(O)$_2$((*E*)-CH=CHPh)(PPr$^i_3$)$_2$] (*d*(Os−O) = 1.70(1), 1.72(1) Å).[11a] The lengthening of the Os−O bond in **5a** is due to the two additional electrons in the $(d_{xy})^2(d_{xz})^1(d_{yz})^1$ configuration as compared to the d^2 osmium(VI) systems. A partial, qualitative correlation diagram (Figure 8) indicates that the degenerate d_{xz} and d_{yz} orbitals have antibonding character with respect to the Os−O bond.[2] Their partial occupation by parallel spins is confirmed by the magnetic data.[2,12d,13b]

Qualitative MO considerations explain further structural features. The Os−Cl bond is much longer in **5a** (2.442(1) Å) than in five-coordinate **3a** (2.371(1) Å) and in the η^2-O_2 complex **4a** (2.380(1) Å). The opposite trend is expected on the basis of the ionic radius contraction upon going from Os(II) to Os(IV). The straightforward explanation is that both the dioxygen complex **4a** and the 16-electron species **3a** are stabilized by $p_\pi \rightarrow d_\pi$ donation from the halide, although via different mechanisms, as discussed above.[25,45] In contrast, **5a** contains two π-donors, a strong one, the oxo ligand,[2] and a much weaker one, the chloro ligand (Figure 8),[25] and the d^4 metal center has two electrons occupying the antibonding d_{xz} and d_{yz} orbitals. This results in a 2-fold five-electron $p_\pi-d_\pi$ destabilizing interaction between the oxo and chloro lone pairs and the half-filled d_{xz} and d_{yz} orbitals of osmium (Figure 8), which possibly explains the longer Os−Cl bond. Although it has been suggested that $p_\pi-d_\pi$ destabilization energies are very small,[46] the present

(44) Marshman, R. W.; Bigham, W. S.; Wilson, S. R.; Shapley, P. A. *Organometallics* **1990**, *9*, 1341.
(45) For examples of π-stabilized 16-electron complexes, see: Barthazy, P.; Hintermann, L.; Stoop, R. M.; Wörle, M.; Mezzetti, A.; Togni, A. *Helv. Chim. Acta* **1999**, *82*, 2448 and references therein.

structural data show that such effects are sizable, at least when a strong donor, such as an oxo ligand, is involved.[47]

Reactivity of *trans*-[OsX(O)(P−P)$_2$]$^+$. Most of the reactions were performed with *trans*-[OsCl(O)(dcpe)$_2$]$^+$ (**5a**), but *trans*-[OsBr(O)(dcpe)$_2$]$^+$ (**5b**) and *trans*-[OsCl(O)(depe)$_2$]$^+$ (**5c**) show very similar reactivity. The oxo complexes **5** do not react with CO (1 atm, 20 °C), transfer oxene to isonitriles, thioethers, and styrene, or react with these substrates in other ways. Stoichiometric oxidation of alcohols does not take place in $CDCl_3$ at room temperature. However, some [OsH$_3$(dcpe)$_2$]$^+$ [37] is formed in refluxing methanol, together with decomposition products. This suggests that the protic solvent is able to protonate the oxygen and reduce the complex under forcing conditions. To test the possibility of reoxygenating the oxo species **5a**, we treated it with H_2O_2 or O_2, but the η^2-O_2 complex **4a** was not formed in either case.

The d^4 osmium oxo complexes reported to date have been prepared by oxidation of the corresponding aquo complexes of the general formula [Os(OH$_2$)N$_5$]$^{2+}$ (N = sp^2 or sp^3 N-donor).[12a−c,f] These species are highly reactive or unstable toward disproportionation to the point that the osmium(IV) oxidation state is sometimes considered as "missing".[12a−c,f] Also, a high reactivity is expected for octahedral d^4 oxo complexes owing to their reduced Os−O bond order (Figure 5).[2] Thus, we were surprised to find that **5a** reacts with nucleophiles (PR_3 and SR_2) sluggishly or does not react at all. Complex **5a** reacts with PPh_3 (in an NMR tube sealed under vacuum to exclude traces of O_2), giving Ph_3PO (20%) and a small amount of **3a** (ca. 5% by ^{31}P NMR), together with other unidentified products after 14 d (eq 3). The ^{1}H NMR spectrum of the reaction solution

$$\textit{trans}\text{-}[OsCl(O)(dcpe)_2]^+ + Ph_3P \rightarrow [OsCl(dcpe)_2]^+ + Ph_3PO \quad (3)$$

indicates that **5a** is still present after this time, but other unidentified paramagnetic complexes are formed. The reaction with PMe_3 is not significantly faster. As a comparison, the d^4 oxo species [Ru(O)(TMP)] (TMP = the 5,10,15,20-tetramesitylporphyrin dianion) readily oxidizes PPh_3 under analogous conditions.[48]

The above results suggest that the dissociation energy of the Os=O bond is lower than 125 kcal mol^{-1}, the dissociation energy of the P−O bond in PPh_3.[49] This appears reasonable also in view of the long Os−O distance (1.834(3) Å) and the presence of two π-antibonding electrons discussed above. Provided that reaction 3 is thermodynamically favored, its low rate points to the existence of a kinetic barrier. As the dcpe and depe analogues **5a** and **5c** react similarly, we suspect that the nature of the kinetic barrier is electronic rather than steric. A possible explanation is that the attack of the incoming nucleophile on the LUMO's of **5**, the degenerate d_{xz} and d_{yz} orbitals, must be preceded by electron pairing (Figure 5).[50] Thus, the attack on complexes **5** requires either geometrical rearrangement or the involvement of the high-energy d_{z^2} orbital.

Although the oxo complexes **5** are not useful oxidants, the discovery of stable phosphine oxo complexes is important, as ruthenium analogues of *trans*-[OsCl(O)(P−P)$_2$]$^+$ have been invoked as intermediates in catalytic olefin epoxidation. It has been suggested that complexes of the type [RuCl(P−P)$_2$]$^+$ and the related [RuCl(PNNP)]$^+$ complexes (PNNP = tetradentate ligands with P and N donors) catalyze the asymmetric epoxidation of olefins with hydrogen peroxide and PhIO as oxidants and with the involvement of oxo species of Ru(IV).[51]

Conclusion

The main reaction of the dioxygen complexes [OsX(η^2-O$_2$)(dcpe)$_2$]$^+$ (**4**) is the loss of one oxygen atom to form *trans*-[OsX(O)(P−P)$_2$]$^+$ (**5**). The reactivity of coordinated dioxygen is analogous to that of peroxide. The investigations concerning the reactivity of the oxo species **5** show clearly that these osmium complexes are much less reactive than their Fe and Ru analogues. This can be qualitatively explained by considering that the metal center becomes softer (and the oxo species less electrophilic) upon going from 3d to 5d metals. This effect is reinforced upon going from iron porphyrins to [RuCl(PNNP)]$^+$ and [OsCl(P−P)$_2$]$^+$ as the ligand set is changed from N$_4$ to P$_2$N$_2$ (a drastic change as the extensive π interactions in the metalloporphyrin are lost) and, finally, to P$_4$. Besides the significance of *trans*-[OsX(O)(P−P)$_2$]$^+$ with respect to nonbiomimetic dioxygen activation, its isolation and characterization lend support to previous mechanistic speculations regarding the catalytic epoxidation of olefins catalyzed by [RuCl(P−P)$_2$]$^+$.

Experimental Section

General Details. All operations were carried out under argon using standard Schlenk techniques or in a glovebox (Braun) under purified nitrogen. Solvents were purified by standard methods. All chemicals used were of reagent grade or comparable purity. 1,2-Bis((2*R*,5*R*)-2,5-dimethylphospholano)benzene (Me-duphos) was purchased from Strem. The ligand dcpe and *trans*-[OsCl$_2$(dcpe)$_2$] were prepared as previously reported (see ref 14). Yields are based on the metal. Infrared spectra were recorded on a Perkin-Elmer Paragon 1000 FT-IR spectrometer, and UV−visible spectra, on a Kontron Instruments Uvikon 922 spectrophotometer. Microanalyses were performed by the Laboratory of Microelemental Analysis at the Organic Laboratories of the ETH Zürich. ^{1}H, ^{13}C{^{1}H}, and ^{31}P{^{1}H} and 2D correlation NMR spectra were obtained with Bruker Avance 250, 300, 400, and 500 spectrometers. ^{1}H (and ^{13}C) and ^{31}P chemical shifts are relative to TMS and external 85% H_3PO_4, respectively. Mass spectrometry was carried out by the Analytic Service of the Organic Laboratories at the ETH Zürich. NaBArF was prepared by a literature method.[52]

***cis*-[OsCl$_2$(depe)$_2$], 2c.** An improved synthesis for **2c** was as follows: [(PEt$_2$Ph)$_3$Os(μ-Cl)$_3$Os(PEt$_2$Ph)$_3$]Cl (1.021 g, 0.672 mmol) and depe (1.24 g, 6.0 mmol) were heated together without solvent for 12 h. The resulting colorless solid was extracted with boiling hexane (50 mL) to remove diethylphenylphosphine. The resulting white microcrystals were filtered off and washed twice with hexane. Yield: 829 mg (92%). ^{1}H NMR ($CDCl_3$): δ 1.0−32.7 (m, 48 H, C*H*$_2$, C*H*$_3$). ^{31}P NMR: δ 19.4 (t, 2 P, $^2J_{PP'}$ = 8.8 Hz), 10.9 (t, 2 P). Other data are as in ref 17.

***cis*-[OsCl$_2$(Me-duphos)$_2$], 2d.** [(PEt$_2$Ph)$_3$Os(μ-Cl)$_3$Os(PEt$_2$Ph)$_3$]Cl (541 mg, 0.356 mmol) and Me-duphos (459 mg, 1.50 mmol, 1.05 equiv) were heated together without solvent for 12 h. Diethylphenylphosphine

(46) Holland, P. L.; Andersen, R. A.; Bergman, R. G. *Comments Inorg. Chem.* **1999**, *21*, 115.
(47) Mayer, J. M. *Comments Inorg. Chem.* **1988**, *8*, 125.
(48) Cheng, S. Y. S.; James, B. R. *J. Mol. Catal. A: Chem* **1997**, *117*, 91.
(49) Data from: Sawyer, D. T. *Oxygen Chemistry*; Oxford University Press: New York, 1991; p 77.
(50) The spin barrier is not present in oxygen transfers from diamagnetic octahedral d^2 systems, as recently discussed for rhenium(V) oxo complexes: Seymore, S. B.; Brown, S. N. *Inorg. Chem.* **2000**, *39*, 325.
(51) (a) Bressan, M.; Morvillo, A. *Inorg. Chem.* **1989**, *28*, 950. (b) Morvillo, A.; Bressan, M. *J. Mol. Catal. A: Chem.* **1997**, *125*, 119. (c) Maran. F.; Morvillo, A.; d'Alessandro, N.; Bressan, M. *Inorg. Chim. Acta* **1999**, *288*, 122. (d) Stoop, R. M.; Bauer, C.; Setz, P.; Wörle, M.; Wong, T. Y. H.; Mezzetti, A. *Organometallics* **1999**, *18*, 5691. (e) Stoop, R. M.; Mezzetti, A. *Green Chem.* **1999**, 39.
(52) Brookhart, M.; Rix, F. C.; DeSimone, J. M.; Barabak, J. C. *J. Am. Chem. Soc.* **1992**, *114*, 5894.

was separated from the resulting pale yellow oil by distillation under reduced pressure at 200 °C. The solid residue was then crushed and vacuum-dried, yielding a pale-yellow powder. Yield: 612 mg (98%). ^{1}H NMR ($CDCl_3$): δ 9.79 (br, 2 H, Ph *H*), 9.58 (br, 2 H, Ph *H*), 9.3 (br, 4 H, Ph *H*), 5.40−5.30 (m, 2 H, C*H*), 4.98−4.78 (m, 6 H, C*H*, CH_2), 4.77−4.59 (m, 2 H, C*H*), 4.41−4.25 (m, 2 H, C*H*), 4.09−3.30 (m, 18 H, CH_2, wherefrom δ 3.73 (dd, 6 H, CH_3, $J_{HH'}$ = 7 Hz, J_{PH} = 14 Hz)), 3.13 (dd, 6 H, CH_3, $J_{HH'}$ = 7 Hz, J_{PH} = 13 Hz), 2.49 (dd, 6 H, CH_3, $J_{HH'}$ = 7 Hz, J_{PH} = 14 Hz), 2.14 (dd, 6 H, CH_3, $J_{HH'}$ = 7 Hz, J_{PH} = 16 Hz). ^{31}P NMR ($CDCl_3$): δ 40.2 (t, 2 P, $^2J_{PP'}$ = 9.0 Hz), 37.5 (t, 2 P). MS (FAB$^+$): *m*/*z* 874 (M^+, 16), 839 ([M − Cl]$^+$, 100). Anal. Calcd for $C_{36}H_{56}Cl_2OsP_4$: C, 49.48; H, 6.46. Found: C, 49.49; H, 6.43.

[OsCl(dcpe)$_2$]BPh$_4$, [3a]BPh$_4$. A simplified synthesis was employed: *trans*-[$OsCl_2$(dcpe)$_2$] (3.04 g, 2.75 mmol) and $TlPF_6$ (960 mg, 2.75 mmol) were suspended in CH_2Cl_2 (50 mL), and the mixture was stirred overnight at room temperature. The thallium chloride that formed was filtered off, Pr^{i}OH (40 mL) was added, and CH_2Cl_2 was removed under vacuum to yield a dark brown precipitate of [**3a**]PF_6. Yield: 2.38 g (71%). A slurry of [**3a**]PF_6 (121.6 mg, 0.10 mmol) and $NaBPh_4$ (171 mg, 0.50 mmol) was stirred for 10 min in CH_2Cl_2 (10 mL). Addition of methanol (40 mL) and evaporation of CH_2Cl_2 under vacuum gave brown [**3a**]BPh_4, which was filtered off and vacuum-dried. Yield: 119 mg (86%). Analytical and spectroscopic data were as reported in ref 14.

[OsBr(dcpe)$_2$]PF$_6$, [3b]PF$_6$. An improved synthesis was again employed: *trans*-[$OsBr_2$(dcpe)$_2$] (4.20 g, 3.5 mmol) and $TlPF_6$ (1.22 g, 3.5 mmol) were suspended in CH_2Cl_2 (50 mL), and the mixture was stirred overnight at room temperature. The thallium bromide that formed was filtered off, Pr^{i}OH (40 mL) was added, and CH_2Cl_2 was removed under vacuum, yielding an almost black precipitate. Yield: 3.99 g (87%).^{31}P NMR ($CDCl_3$): δ 40.8 (t, 2 P, $^2J_{PP'}$ = 1.8 Hz), 26.7 (t, 2 P, $^2J_{PP'}$ = 1.8 Hz). Analytical data were as in ref 14.

[OsCl(Me-duphos)$_2$]PF$_6$, [3d]PF$_6$. Complex **2d** (87 mg, 0.1 mmol) was dissolved in CH_2Cl_2 (10 mL), $TlPF_6$ (34 mg, 0.15 mmol) was added, and the solution was stirred overnight. TlCl was then filtered off, and Pr^{i}OH (20 mL) was added. Evaporation of CH_2Cl_2 under vacuum afforded red microcrystals. Yield: 71 mg (72%). ^{1}H NMR ($CDCl_3$): δ 7.85 (br, 2 H, Ph *H*), 7.54−7.33 (m, 6 H, Ph *H*), 3.24 (s br, 2 H, C*H*), 3.08 (br, 2 H, C*H*), 2.48−2.32 (m, 4 H, C*H*), 2.20−2.03 (m, 8 H, CH_2), 1.94−1.53 (m, 8 H, CH_2), 1.47 (dd, 6 H, CH_3, $J_{HH'}$ = 8 Hz, J_{PH} = 18 Hz), 1.28 (dd, 6 H, CH_3, $J_{HH'}$ = 7 Hz, J_{PH} = 17 Hz), 0.45 (dd, 6 H, CH_3, $J_{HH'}$ = 7 Hz, J_{PH} = 14 Hz), 0.27 (dd, 6 H, CH_3, $J_{HH'}$ = 7 Hz, J_{PH} = 15 Hz). ^{31}P NMR ($CDCl_3$): δ 76.1 (t, 2 P, $^2J_{PP'}$ = 5.5 Hz), 42.6 (t, 2 P), −143 (septet, 1 P, PF_6, $^1J_{PF}$ = 710 Hz). MS (FAB$^+$): *m*/*z* 839 (M^+, 100), 755 ([M − C_6H_{12}]$^+$, 8). Anal. Calcd for $C_{36}H_{56}ClF_6OsP_5$: C, 43.97; H, 5.74. Found: C, 43.71; H, 5.91.

[OsCl(η^2-O$_2$)(dcpe)$_2$]BPh$_4$, [4a]BPh$_4$. A slurry of [**3a**]PF_6 (0.846 g, 0.70 mmol) and $NaBPh_4$ (1.195 g, 3.5 mmol) in CH_2Cl_2 (50 mL) and Pr^{i}OH (10 mL) was stirred for 10 min, after which more Pr^{i}OH (100 mL) was added. CH_2Cl_2 was then removed under vacuum, and the precipitate was filtered off and dissolved in CH_2Cl_2/Pr^{i}OH (200 mL, 1:1 v/v). This solution was stirred under O_2 (1 atm) at room temperature for 1 h. The CH_2Cl_2 was then removed under vacuum, and the resulting light green [**4a**]BPh_4 was filtered off. Yield: 0.751 g (87%). The presence of CH_2Cl_2 (0.5 equiv) was supported by ^{1}H NMR spectroscopy. ^{1}H NMR ($CDCl_3$): δ 7.39 (s, 8 H, Ph *H*), 7.09 (t, 8 H, Ph *H*, $J_{HH'}$ = 7.4 Hz), 6.93 (t, 4 H, Ph *H*, $J_{HH'}$ = 7.1 Hz), 2.5−2.2 (m, 12 H, PCH_2, PC*H*), 2.2−1.7 (m, 44 H, C_6H_{11}), 1.7−1.2 (m, 40 H, C_6H_{11}). ^{31}P NMR ($CDCl_3$): δ −4.0 (s, 4 P). UV−vis (CH_2Cl_2) λ_{max}, nm (ϵ_{max}, M^{-1} cm^{-1}): 345 (sh), 435 (sh). MS (FAB$^+$): *m*/*z* 1104 ([M + H]$^+$, 54), 1087 ([M − O]$^+$, 100), 1071 ([M − 2O]$^+$, 11), 921 ([M − O − 2C_6H_{11}]$^+$, 14), 665 ([M − O − dcpe]$^+$, 8). Anal. Calcd for $C_{76}H_{116}BCl_3O_2OsP_4$·0.5$CH_2Cl_2$: C, 62.74; H, 8.05. Found: C, 62.87; H, 8.09.

[OsBr(η^2-O$_2$)(dcpe)$_2$]BPh$_4$, [4b]BPh$_4$. A CH_2Cl_2 solution of [OsBr(dcpe)$_2$]PF_6 (56.3 mg, 45 μmol) was stirred under an O_2 atmosphere for 3 h, after which Pr^{i}OH (30 mL) and $NaBPh_4$ (70 mg, 200 μmol) in CH_2Cl_2 (20 mL) were added. CH_2Cl_2 was removed under vacuum, and the resulting precipitate was filtered off and vacuum-dried. Yield: 56 mg (85%). ^{1}H NMR ($CDCl_3$): δ 7.85 (s, 8 H, Ph *H*), 7.4−7.3 (m, 8 H, Ph *H*), 7.1−7.0 (m, 4 H, Ph *H*), 2.4−0.9 (m, 96 H, PCH_2, PC*H*, C_6H_{11}). ^{31}P NMR: δ −8.6 (s, 4 P). MS (FAB$^+$): *m*/*z* 1148 ([M + H]$^+$, 100), 1131 ([M − O]$^+$, 48), 1115 ([M − 2O]$^+$, 20), 965 ([M − O − 2C_6H_{11}]$^+$, 4), 709 ([M − O − dcpe]$^+$, 8). Anal. Calcd for $C_{76}H_{116}BBrO_2OsP_4$: C, 62.24; H, 7.97; O, 2.18. Found: C, 62.27; H, 8.11; O, 2.46.

[OsCl(η^2-O$_2$)(depe)$_2$]PF$_6$, [4c]BPh$_4$. Complex **2c** (67 mg, 0.1 mmol) and $TlPF_6$ (35 mg, 0.1 mmol) were dissolved in MeOH (10 mL). After 10 min of stirring, the TlCl that formed was filtered off, the volume of the solution was reduced under vacuum, and hexane (10 mL) was added. The resulting precipitate was then filtered off and treated with $NaBPh_4$ as described for [**4b**]BPh_4. Yield: 49 mg (60%). This substance contained traces of [**5c**]BPh_4. ^{1}H NMR ($CDCl_3$): δ 2.54−1.85 (m, 24 H, CH_2), 1.55−0.86 (m, 24 H, CH_3). ^{31}P NMR: δ 9.6 (s, 4 P). MS (FAB$^+$): *m*/*z* 671 (M^+, 95), 656 ([M − O + H]$^+$, 64), 640 ([M − 2O + H]$^+$, 100), 205 ([depe − H]$^+$, 10). Anal. Calcd for $C_{44}H_{68}BClO_2OsP_4$: C, 53.42; H, 6.93. Found: C, 53.52; H, 6.89.

***trans*-[OsCl(O)(dcpe)$_2$]PF$_6$, [5a]PF$_6$.** [**3a**]PF_6 (1.286 g, 1.06 mmol) was dissolved in CH_2Cl_2 (50 mL) and Pr^{i}OH (100 mL), and the solution was was stirred in air for 2 d. Evaporation of the CH_2Cl_2 under vacuum yielded [**5a**]PF_6 as a light brown solid. Yield: 1.04 g (80%). ^{1}H NMR: see Table 2. ^{31}P NMR ($CDCl_3$): δ −143 (septet, 1 P, PF_6, $^1J_{PF}$ = 710 Hz). MS (FAB$^+$): *m*/*z* 1087 (M^+, 100), 1071 ([M − O]$^+$, 12), 921 ([M − 2C_6H_{11}]$^+$, 19), 665 ([M − dcpe]$^+$, 9). Anal. Calcd for $C_{52}H_{96}ClF_6OOsP_5$: C, 50.70; H, 7.85; O, 1.30; Cl, 2.88. Found: C, 50.46; H, 7.99; O, 1.53; Cl, 3.09.

***trans*-[OsCl(O)(dcpe)$_2$]BPh$_4$, [5a]BPh$_4$.** [**5a**]PF_6 (123.1 mg, 0.10 mmol) and $NaBPh_4$ (171 mg, 0.50 mmol) were dissolved in CH_2Cl_2 (10 mL). Addition of CH_3OH (40 mL) and evaporation of CH_2Cl_2 under vacuum yielded a light brown precipitate, which was filtered off and vacuum-dried. Yield: 125 mg (89%). ^{1}H NMR ($CDCl_3$): δ 7.39 (s, 8 H, Ph *H*), 7.09 (t, 8 H, Ph *H*, $J_{HH'}$ = 7.4 Hz), 6.93 (t, 4 H, Ph *H*, $J_{HH'}$ = 7.1 Hz); for **5a** data, see Table 2. UV−vis (CH_2Cl_2) λ_{max}, nm (ϵ_{max}, M^{-1} cm^{-1}): 350 (2200), 410 (sh), 480 (sh), 575 (sh). MS (FAB$^+$): *m*/*z* 1087 (M^+, 100), 1071 ([M − O]$^+$, 12), 921 ([M − 2C_6H_{11}]$^+$, 19), 665 ([M − dcpe]$^+$, 9). Anal. Calcd for $C_{76}H_{116}BClOOsP_4$: C, 64.92; H, 8.31; O, 1.14; Cl, 2.52. Found: C, 64.74; H, 8.38; O, 1.13; Cl, 2.43.

***trans*-[OsBr(O)(dcpe)$_2$]BArF, [5b]BArF.** [**3b**]PF_6 (1.00 g, 0.80 mmol) was dissolved in CH_2Cl_2 (50 mL), and the solution was stirred in air for 2 d. The resulting complex [OsBr(η^2-O_2)(dcpe)$_2$]PF_6 was treated with gaseous HCl for 1 min. After 12 h of stirring, the mixture was filtered, and the filtrate was treated with NaBArF (710 mg, 0.80 mmol). Addition of ^{i}PrOH (100 mL) and removal of CH_2Cl_2 under vacuum gave a brown product. Yield: 1.03 g (66%). ^{1}H NMR ($CDCl_3$): δ 7.79 (s, 8 H, Ph *o-H*), 7.63 (s, 4 H, Ph *p-H*); for **5b** data, see Table 2. MS (FAB$^+$): *m*/*z* 1131 (M^+, 100), 1115 ([M − O]$^+$, 84), 1049 ([M − HBr]$^+$, 31), 965 ([M − 2C_6H_{11}]$^+$, 27). Anal. Calcd for $C_{84}H_{108}BBrF_{24}OOsP_4$: C, 49.63; H, 5.35. Found: C, 49.63; H, 5.19.

***trans*-[OsCl(O)(depe)$_2$]PF$_6$, [5c]BPh$_4$.** This complex was prepared similarly to [**4c**]BPh_4, but stirring was prolonged to 12 h before filtration and precipitation. Yield: 67 mg (84%). ^{1}H NMR: see Table 2. ^{31}P NMR δ −143 (septet, 1 P, PF_6, $^1J_{PF}$ = 710 Hz). MS (FAB$^+$): *m*/*z* 656 ([M + H]$^+$, 100). Anal. Calcd for $C_{44}H_{68}BClOOsP_4$: C, 54.29; H, 7.04. Found: C, 54.22; H, 6.88.

Oxidation of Iodide with [4a]BPh$_4$. A CH_2Cl_2 solution of [**4a**]BPh_4 (0.2 mM, 1 mL) and a CH_2Cl_2 solution of [NBu_4]I (2.0 mM, 1 mL) were mixed in a UV cuvette. The reaction was initiated by the addition of one drop of a saturated solution of anhydrous HCl in CH_2Cl_2. The spectrum of the reaction solution recorded immediately after the addition and corrected for the absorbance of **5a** indicated that $[I_3]^-$ was formed on the basis of the reference for the triiodide ion. Quantitative conversion (within experimental error) was calculated from absorbance data at 365 nm. Two measurements gave the same results. No reaction occurred without addition of acid. Blank experiments omitting HCl gave no reaction.

X-ray Structure Determinations. Crystals of [OsCl(dcpe)$_2$]PF_6 ([**3a**]PF_6), [OsBr(dcpe)$_2$]PF_6 ([**3b**]PF_6), [OsCl(η^2-O_2)(dcpe)$_2$]BPh_4 ([**4a**]BPh_4), and *trans*-[OsCl(O)(dcpe)$_2$]BPh_4 ([**5a**]BPh_4) were obtained by slow evaporation of concentrated CH_2Cl_2/Pr^{i}OH solutions of the respective complexes. Crystals of [**3a**]PF_6 and [**3b**]PF_6 were grown in a glovebox under purified N_2. Data were collected on a Siemens CCD SMART area detector system equipped, except for the [**3b**]PF_6 study

(four-circle diffractometer Syntex $P2_1$), with a normal-focus Mo-target X-ray tube. Unit cell dimension determinations and data reductions were performed by standard procedures. An empirical absorption correction (SADABS) was applied for **3a**, **4a**, and **5a**. The structures were solved with SHELXS-96 using direct methods and refined by full-matrix least-squares calculations based on F^2 with anisotropic displacement parameters for all non-H atoms. Disordered atoms were refined isotropically. Hydrogen atoms (bound to nondisordered C atoms) were introduced at calculated positions and refined with a riding model using individual isotropic thermal parameters for each group. Further details of the crystallographic determinations are given in the Supporting Information.

Maximum and minimum difference peaks for [**3a**]PF_6 were +0.71 and −0.55 e Å^{-3}; the largest and the mean Δ/σ values were −0.638 and +0.007. In [**3b**]PF_6, cyclohexyl C(15)−C(20) is disordered and was split between two chair conformations with 64:36 refined occupancies. Maximum and minimum difference peaks were +3.834 and −1.907 e Å^{-3} (at 1.18 Å from Os); the largest and the mean Δ/σ values were −0.002 and 0.000. In [**4a**]BPh_4, cyclohexyl C(27)−C(32) is disordered and was split between two conformations with 7:3 refined occupancies. Maximum and minimum difference peaks were +1.765 and −1.851 e Å^{-3}; the largest and the mean Δ/σ values were +0.014 and 0.000. In [**5a**]BPh_4, cyclohexyl C(47)−C(52) and phenyl C(71)−C(76) are disordered and were split between two conformations with equal refined occupancies and isotropic displacement parameters. Complete results are reported in the Supporting Information.

Supporting Information Available: A listing of NMR data for **5a** and **5b**, an ORTEP drawing of **3b**, and tables of crystal data, X-ray experimental details, atomic coordinates, thermal parameters, bond distances, and bond angles along with X-ray crystallographic files, in CIF format, for [**3a**]PF_6, [**3b**]PF_6, [**4a**]BPh_4, and [**5a**]BPh_4. This material is available free of charge via the Internet at http://pubs.acs.org.

IC0002420